CHEMISTRY
A EUROPEAN JOURNAL

DOI: 10.1002/chem.200501174

The Synthesis and Characterization of all Diastereomers of a Linear Symmetrically Fused Tris-Tröger's Base Analogue: New Chiral Cleft Compounds

Josep Artacho, Patrik Nilsson, Karl-Erik Bergquist, Ola F. Wendt, and Kenneth Wärnmark*[a]

Abstract: The synthesis and characterization of all diastereomers of a linear symmetrically fused tris-Tröger's base analogue are described. The diastereomers are unambiguously assigned as *syn–anti* **1a**, *anti–anti* **1b**, and *syn–syn* **1c** isomers, by using X-ray diffraction analysis and NMR spectroscopy. For the first time, the *anti–anti* and the *syn–syn* diastereomers of a linear symmetrically fused tris-Tröger's base analogue have been synthesized. Molecules **1a** and **1c** are new cleft compounds and analysis of compound **1a** in the solid state shows inclusion of one molecule of CH_2Cl_2 in the larger aromatic cleft, whereas in isomer **1c** disordered solvent molecules are trapped in the extended aromatic cleft. Furthermore, in the solid state, isomer **1c** forms infinite open channels along one of the crystallographic axes and perpendicular to this axis there are infinitely extending "wedged-ravines". Importantly, each of the diastereomers **1a–c** is resistant to inversion at the stereogenic nitrogen atoms under strongly and weakly acidic conditions in the range from room temperature (RT) to 95 °C. This observed configurational stability at the stereogenic nitrogens of **1a–c** is unique for analogues of Tröger's base in general to date. Finally, the ratio of cleft compounds **1a** and **1c** significantly increased relative to cavity compound **1b** when ammonium chloride was used as an additive in the Tröger's base condensation to **1a–c** suggesting a templating effect of the ammonium ion.

Keywords: chirality · cleft compound · inclusion compounds · isomerization · Tröger's base · X-ray diffraction

Introduction

Molecular recognition phenomena are central to virtually all life processes and the development of artificial receptors is one means of gaining a deeper understanding of host–guest interactions. Particularly challenging is the understanding of the recognition processes of relatively unfunctionalized molecules. Such processes take place on concave surfaces and involve mainly nondirectional solvophobic effects[1] and van der Waals interactions.[2] If the surface is aromatic, additional interactions, such as aromatic stacking[3] and cation–π interactions[4] between the surface of the receptor and the ligand, are feasible. Synthetic molecules with *extended* concave aromatic surfaces are generally called molecular cleft compounds and are often referred to as tweezers or clips depending on whether a guest is bound at the tip of the cleft (tweezer) or deeper inside (clip).[5] Achiral molecular tweezers and clips have been constructed by Whitlock,[6a] Zimmermann,[6b] Nolte,[6c,d] Klärner,[5,6e,f] and Fukazawa[6g] and their respective co-workers. Notably, there are very few chiral molecular cleft compounds, however, some based on Kagan's ether have been synthesized by Harmata.[7] In the quest for chiral molecular cleft compounds, attention has been drawn to the C_2-symmetric Tröger's base, 2,8-dimethyl-6*H*,12*H*-5,11-methanodibenzo[*b*,*f*][1,5]diazocine (see Figure 1), which owes its chirality to the presence of two configurationally stable stereogenic nitrogen atoms.[8] This synthetic molecule possesses a relatively rigid chiral concave aromatic surface, making it a good structural motif as a synthetic receptor for relatively unfunctionalized molecules. The Tröger's base motif has mainly been used as a scaffold to anchor recognition elements in synthetic receptors for

[a] J. Artacho, P. Nilsson, Dr. K.-E. Bergquist, Dr. O. F. Wendt, Dr. K. Wärnmark
Organic Chemistry, Department of Chemistry
Lund University, 221 00 Lund (Sweden)
Fax: (+46) 46-222-4119
E-mail: Kenneth.Warnmark@organic.lu.se

Supporting information for this article is available on the WWW under http://www.chemeurj.org/ or from the author.

WILEY InterScience DISCOVER SOMETHING GREAT
© 2006 Wiley-VCH Verlag GmbH & Co. KGaA, Weinheim

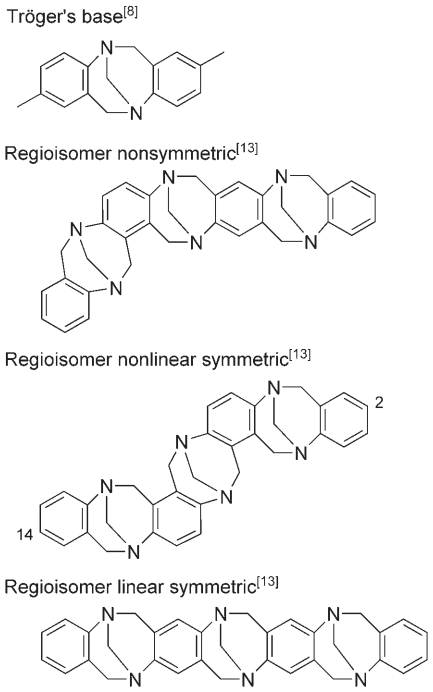

Figure 1. Structure of Tröger's base and the possible extended-regioisomers of fused tris-Tröger's base analogues.

functionalized molecules.[9] However, Wilcox and co-workers pioneered the incorporation of the Tröger's base framework in chiral molecular cleft compounds by fusing the methano–diazocine core of one Tröger's base unit with two bicyclic aromatic building blocks to attempt to find analogues of Tröger's base that could act as receptors for unfunctionalized molecules using the concave aromatic surface.[10] The first molecule containing two fused Tröger's base analogues was first synthesized by Pardo et al.[11a,c] and later by Král et al.[11b] Those groundbreaking publications were followed up by Král et al.[11b,12b] and Pardo et al.,[12a,d] and somewhat later by us[12c] in the synthesis of fused tris-Tröger's base analogues.

Generally there are three possible regioisomers of fused tris-Tröger's base analogues, the nonsymmetric, the nonlinear-symmetric, and the linear-symmetric regioisomers (see Figure 1).[13]

In addition, for each of these regioisomers there are three different possible diastereomers, *syn–anti*, *anti—anti*, and *syn–syn*.[14a,b] Those diastereomers are shown in Scheme 1, compounds **1a**–**c**, for a linear-symmetric regioisomer of a fused tris-Tröger's base analogue. However, it is only the *syn–syn* diastereomer of fused tris-Tröger's base analogues and to a lesser extent the *syn–anti* diastereomer that possesses an extended cleft; the *anti—anti* just possesses two cavities. To date it is only for the nonlinear-symmetric regioisomer of the fused tris-Tröger's base analogue synthesized by Pardo et al., that the *syn–syn* diastereomer has been isolated and unambiguously characterized, thus constituting the only fused tris-Tröger's base to date possessing an extended aromatic chiral cleft.[12a,d] To make cleft molecules

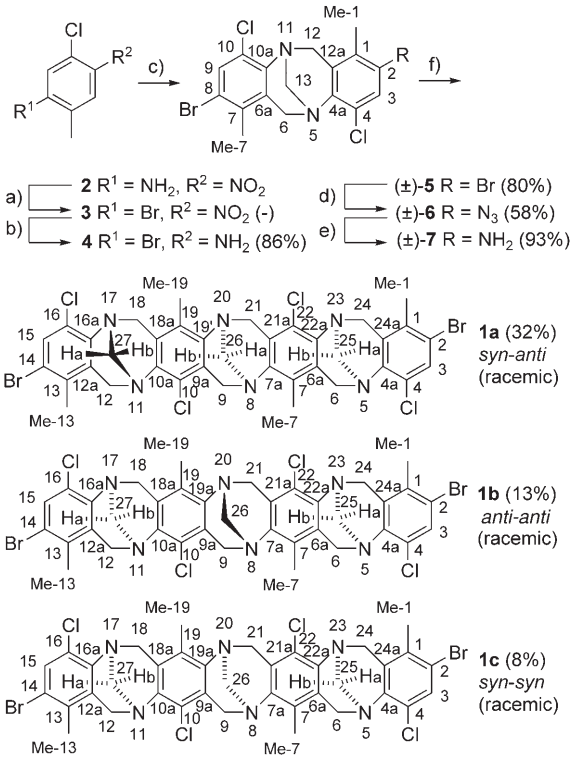

Scheme 1. The synthesis route to linear symmetrically fused tris-Tröger's base analogues **1a**–**c**. a) Aqueous HBr (48% v/v), AcOH (glacial), $NaNO_2$, 85°C; b) $SnCl_2$, EtOH, 70°C; c) paraformaldehyde, TFA (conc.), −10°C; d) *n*BuLi, THF, TsN_3, −78°C; e) $NaBH_4$, THF, RT; f) paraformaldehyde, TFA (conc.), −10°C.

more extended, having tubular-shape based on higher generations of fused Tröger's base analogues, it is necessary to use the *syn–syn* diastereomer of a linear-symmetric regioisomer of a fused tris-Tröger base analogue as a building block and not the *syn–syn* diastereomer of a nonsymmetric or a nonlinear-symmetric regioisomer as revealed by molecular modelling.[15] Tubular structures are important in the synthesis of organic nanotubes for applications such as in the fields of electronic devices, catalysis, and transport.[16]

We now want to report on the first synthesis, isolation, and characterization of all three diastereomers of a linear symmetrically fused tris-Tröger's base analogue, *syn–anti* (**1a**), *anti–anti* (**1b**), and *syn–syn* (**1c**) (Scheme 1), together with their solid-state structures and their unexpected configurational stability under acidic conditions.[17,18]

Results and Discussion

Synthesis of compounds 1a–c: We have recently published a desymmetrization route to fused Tröger's base analogues that allows the extension of the synthesis of fused tris-Tröger's base analogues to higher generations.[12c] In that work we reported the synthesis, isolation, and characterization of the first *anti–anti* diastereomer of a fused tris-Tröger's base analogue as a nonlinear-symmetric regioisomer.[12c,19] The synthesis of the linear symmetrically fused tris-Tröger's base

 © 2006 Wiley-VCH Verlag GmbH & Co. KGaA, Weinheim

analogues **1a–c** in the present study is based on the same desymmetrization concept. The synthesis route to **1a–c** is shown in Scheme 1 and starts from commercially available 5-chloro-2-methyl-4-nitroaniline (**2**) that is converted to 2-bromo-4-chloro-5-nitrotoluene (**3**)[20] through diazotation in HBr.

The nitro group in compound **3** was reduced by $SnCl_2$ to give 4-bromo-2-chloro-5-methylaniline (**4**). The aniline **4** was one of the key components. The chlorine atom in aniline **4** is positioned in the benzene ring to: 1) allow the formation of only one regioisomer in the two Tröger's base condensations to follow,[17] 2) together with the bromine atom to increase the electronic density of compound **1**, thus facilitating the X-ray diffraction analysis, and 3) together with the methyl group of aniline **4** to increase the solubility of compound **1** in organic solvents. Thus, condensation of aniline **4** under the conditions we developed for the synthesis of halogenated Tröger's base analogues, paraformaldehyde in TFA at −10 °C,[21] afforded the linear C_2-symmetric Tröger's base dibromo analogue **5** as the only regioisomer. This compound was desymmetrized by applying our published conditions[12c] by subjecting it to a single bromine exchange followed by quenching with TsN_3. The resulting 2-azido-8-bromo Tröger's base analogue **6** was reduced by $NaBH_4$ yielding the 2-amino-8-bromo Tröger's base analogue **7**. Reaction of compound **7** with paraformaldehyde in concentrated TFA afforded the linear symmetrically fused tris-Tröger's base analogue **1** as the only regioisomer in a diastereomeric ratio of 53:34:13 (**1a**:**1b**:**1c**) when the TFA was added at −10 °C. This ratio was only affected to a minor extent by adding the TFA at 0 and 10 °C (Table 1), whereas the yield decreased a little.[22] Interestingly, conducting the reaction at −10 °C in the presence of 10 equivalents of NH_4Cl led to an increase in the ratio of the diastereomers containing a cleft, **1a** and **1c**, compared to the cavity compound **1b**, with no decrease in total yield, suggesting a templating effect of the ammonium ion (Table 1). After removal of the TFA in vacuo and addition of aqueous NH_3, the resulting aqueous phase was extracted first with CH_2Cl_2 followed by CC, giving separately the *syn–anti* diastereomer **1a** and the *syn–syn* diastereomer **1c**. These compounds were further purified by using reprecipitations (**1a**) and preparative TLC (**1c**). The remaining aqueous phase was then extracted with $CHCl_3$ giving the *anti–anti* diastereomer **1b**.

Table 1. The product distribution of isomers **1a–c** under different reaction conditions.[a]

Temperature during TFA addition [°C]/additive	Product ratio **1a**:**1b**:**1c**[b]
−10/none	53:34:13
0/none	52:34:14
10/none	50:34:16
−10/NH_4Cl (10 equiv)	60:19:21

[a] Standard conditions. To compound **7** (430 mg, 1.04 mmol), paraformaldehyde (80 mg, 2.7 mmol), and additive at −10, 0, or 10 °C was added TFA (3 mL) over 20 min. The reaction was left at addition temperature for 40 min and was then left at room temperature for 72 h. [b] As determined by ^1H NMR spectroscopy on the crude product mixture.

In principle the compounds **1a–c** could be used to synthesize extended analogues by repeating the desymmetrization methodology described above.

Structure elucidation and solid-state structure of compounds 1a and 1c: Each of the diastereomers **1a** (C_1-symmetric), **1b** (C_2-symmetric), and **1c** (C_2-symmetric) could easily be assigned to fused tris-Tröger's base analogues by NMR spectroscopy and high-resolution mass spectrometry, and in addition, the presence of chloro and methyl substituents as blocking units in the starting mono-Tröger's base compound **7**, ensured that diastereomers **1a–c** are uniquely linear-symmetric regioisomers. Furthermore, the diastereomer **1a** must be *syn–anti* because that is the only C_1-symmetric diastereomer of the linear-symmetric tris-Trögers base analogues **1** and its ^{13}C NMR spectrum contains resonances for all the 37 carbon atoms in the molecule. The ^{13}C NMR spectrum of diastereomers **1b** and **1c**, respectively, both C_2-symmetric diastereomers, contains 19 resonances as expected, and both **1b** and **1c** could either be the *anti–anti* or the *syn–syn* diastereomer. Due to the inherent lack of correlating protons between the different Tröger's base units in diastereomers **1b** and **1c** (as well as in **1a**), NMR spectroscopy could not directly be used in the assignment of diastereomers. Instead, X-ray diffraction analysis of diastereomer **1c** was performed.

Crystals suitable for X-ray diffraction analysis of diastereomer **1c** were obtained by carefully adding Et_2O (0.5 mL) to a solution of compound **1c** in $CDCl_3$ (1 mL) to obtain two layers. The Et_2O layer was allowed to slowly diffuse into the $CDCl_3$ layer and the resulting mixture of solvents was allowed to slowly evaporate resulting in small colorless needles of diastereomer **1c** belonging to the monoclinic space group *P*2/*n*. The X-ray diffraction analysis unambiguously allowed us to assign compound **1c** as the *syn–syn* diastereomer (Figure 2). In the center of the aromatic cavity as defined by the aromatic planes A, B, C, and D, disordered solvent molecule(s) is(are) situated as indicated by the presence of residual electron density after all atoms were located in the Fourier map. The size of the cavity is 8.48(1), 8.59(1), and 9.03(1) Å as defined by the distances between the center of the planes A and C, B and D, and A and D, respectively. The intramolecular dihedral angles between the planes A and B, B and C, and C and D, constituting the cavity, are 105 ± 2, 112 ± 2, and 114 ± 2°, respectively. Those values significantly deviate from the intramolecular dihedral angles of *rac*-Tröger's base itself, 93 and 97°, respectively, for each of the two crystallographically independent molecules.[23]

The intermolecular aggregation of diastereomer **1c** in the solid state is depicted in a view along the crystallographic *b* axis as shown in Figure 3. The unit cell consists of four molecules related to each other by symmetry. Each **1c** isomer is perfectly aligned to another edge-to-edge, with a distance between the chlorines and benzylic amine carbons of 3.9–

 © 2006 Wiley-VCH Verlag GmbH & Co. KGaA, Weinheim

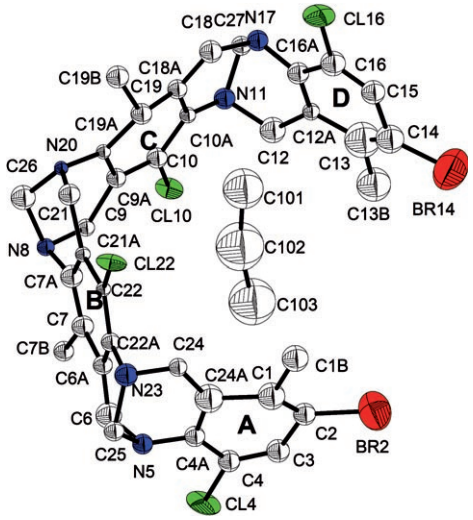

Figure 2. DIAMOND[24] drawing with atomic numbering of **1c**·C_3. Disordered solvent molecule(s) (tentatively labeled C101–C103 and also C_3) is (are) captured in the aromatic cavity. Hydrogen atoms are omitted and thermal ellipsoids are shown at 30% probability.

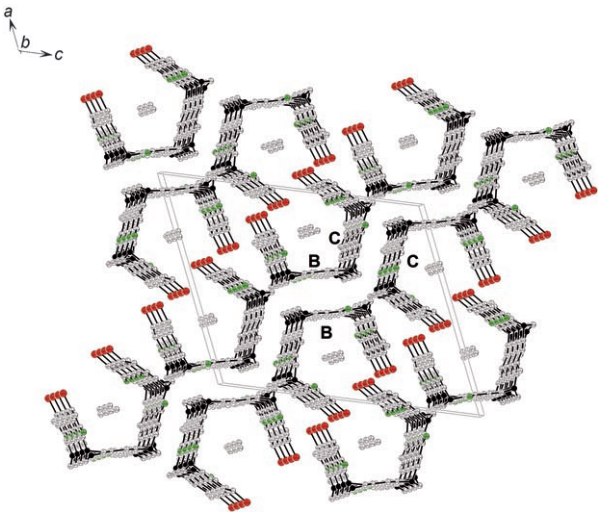

Figure 3. DIAMOND[24] packing diagram of the unit cell of isomer **1c**·C_3. View along the crystallographic *b* axis showing the extended open channels comprising the cavity of isomer **1c** in which disordered solvent molecules (C_3) are residing. Perpendicular to the *b* axis are infinite "wedged-ravines" built up by walls of edge-to-edge aggregated aromatic surfaces B and C, respectively. Hydrogen atoms are omitted and non-hydrogen atoms are shown isotropically.

4.0 Å (CL16···C12, CL10···C18, CL22···C6, and CL4···C24), suggesting weak hydrogen bonds[25] consisting of four C–Cl···H–CH(N)Ph interactions, as one component responsible for the observed alignment of diastereomer **1c** in the solid state. This results in infinite open-channels along the crystallographic *b* axis constituting the cleft of diastereomer **1c**. The cleft contains one or more disordered solvent molecules. Moreover, two such channels are pair-wise aligned to each other with the openings towards each other in such a way that one tip of one cleft-channel is partly inside the opening of the other cleft-channel cleft and vice-versa, the full penetration being hampered by the presence of solvent molecule(s), a situation previously observed for a chiral tweezer molecule based on Kagan's ether.[7a] In the plane perpendicular to the *b* axis "wedged-ravines" are formed that infinitely extend along the crystallographic *b* axis as well as in the perpendicular plane (see Figure 3). Each "wedged-ravine" consists of two types of parallel aromatic wall. One is defined by the *exo* part of the aromatic plane C of diastereomer **1c**, which has an almost perfect π-overlap with aromatic plane C in a neighboring **1c** diastereomer at a distance of 3.9 Å. The other is defined by the *exo* part of the aromatic plane B of diastereomer **1c**, which, in this case, has the π system considerably displaced in parallel from the aromatic plane B in a neighboring diastereomer **1c** to interact with each other by π-stacking. The distance between the two parallel walls is still 3.9 Å, probably indicating van der Waals interactions.

The assignment of **1a** to the *syn–anti* diastereomer based on ^{13}C NMR spectroscopy above was confirmed by an X-ray diffraction analysis of crystals of diastereomer **1a** obtained directly from one of the fractions from CC containing diastereomer **1a**, that was allowed to slowly evaporate resulting in small colorless needles of compound **1a** belonging to the triclinic space group $P\bar{1}$ (Figure 4). One molecule of CH_2Cl_2 is stacked in the extended aromatic cavity as defined by the

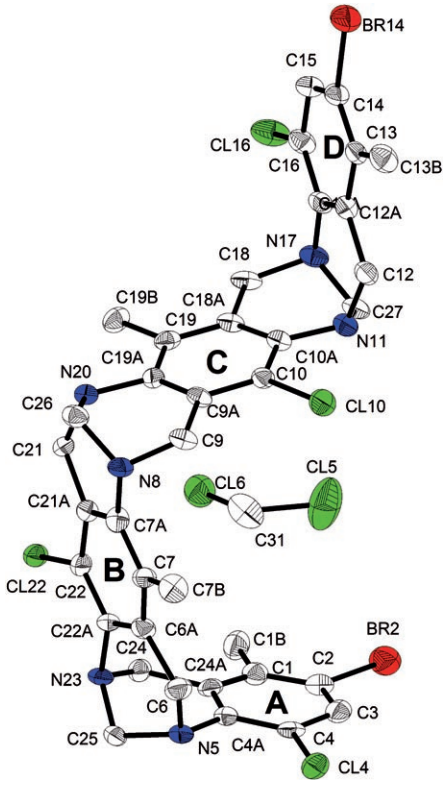

Figure 4. DIAMOND[24] drawing with atomic numbering of isomer **1a**·2CH_2Cl_2. One molecule of CH_2Cl_2 (labeled CL5-C31-CL6) is captured in the larger cavity as defined by aromatic planes A, B, and C. Hydrogen atoms and one molecule of intermolecular CH_2Cl_2 are omitted. Thermal ellipsoids are shown at 30% probability.

 © 2006 Wiley-VCH Verlag GmbH & Co. KGaA, Weinheim

aromatic planes A, B, and C in such a way that the Cl-C-Cl plane is situated more or less at van der Waals distances to the two parallel aromatic planes A and C, 4.12(1) and 3.51(1) Å, respectively. In addition the two hydrogen atoms of CH_2Cl_2 are pointing towards the central aromatic moiety, B, in the extended cavity, placing the carbon of CH_2Cl_2 at a 3.54(1) Å distance to plane B, suggesting two weak CH-aromatic interactions. The intramolecular dihedral angle between the planes A and B, B and C, and C and D, constituting the cavity, are 101 ± 2, 101 ± 2, and $102\pm2°$. Those values deviate from the intramolecular dihedral angle of *rac*-Tröger's base itself (see above) but are smaller than in diastereomer **1c** indicating a smaller intermolecular interaction in the *syn–anti* **1a** than in the *syn–syn* **1c** diastereomer. The size of the extended aromatic cavity is 7.58(1) Å as defined by the distance between the planes A and C.

The intermolecular aggregation of diastereomer **1a** in the solid state is depicted in a view along the crystallographic *a* axis as shown in Figure 5. The unit cell consists of two molecules related to each other by a crystallographic inversion center in such a way that the aromatic plane B of diastereomer **1a** in one molecule is partly overlapping with plane B of a symmetry-related diastereomer **1a** at a van der Waals distance of 3.85(2) Å. In addition to the one molecule of CH_2Cl_2 stacked in the cavity of diastereomer **1a**, another one is situated between each set of symmetry-related molecules in the vicinity of aromatic ring D.

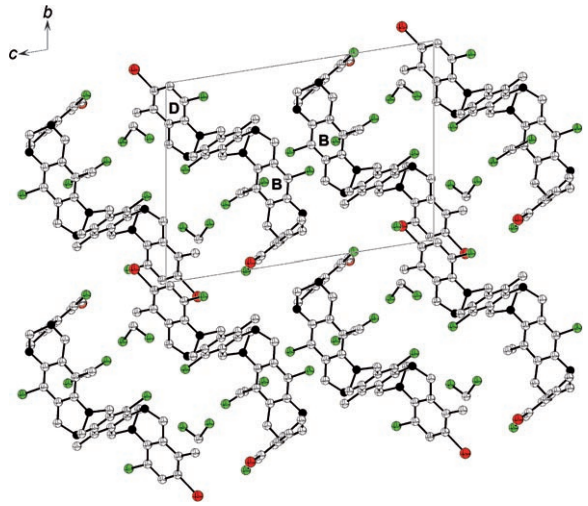

Figure 5. DIAMOND[24] packing diagram of the unit cell of isomer **1a**·2 CH_2Cl_2. The two symmetry-related molecules have partly overlapping aromatic systems B at van der Waals distance. Two molecules of CH_2Cl_2 reside in the unit cell in different positions, one inside the extended aromatic cavity of isomer **1a** and one outside, close to aromatic ring D. Hydrogen atoms are omitted and all atoms are shown isotropically.

Structure elucidation of compound 1b: Despite extensive efforts to grow crystals of compound **1b**, none suitable for X-ray diffraction analysis were obtained. Based on exclusion, the third remaining diastereomer, the *anti–anti*, must be **1b**. This could now be unambiguously confirmed by NMR spectroscopy based on the correlation between the assigned structures of diastereomers **1a** and **1c**, being the *syn–anti* and *syn–syn* isomer, respectively, according to the X-ray diffraction analysis and their corresponding NMR data as outlined below.

Full assignment of NMR chemical shifts was made for compounds **1a**, **1b**, and **1c** using the same strategy as in previous work on fused tris-Trögers base analogues (see Experimental Section).[12c,26] However, it was not possible to use NOE interactions or homoallylic couplings to ascertain the stereochemistry in these linear symmetrically fused tris-Trögers base analogues, as has been the case with nonlinear symmetrically fused tris-Trögers base analogues. Instead, we applied previous observations that the difference in chemical shift between *exo* and *endo* protons in the benzylic methylenes increases due to anisotropy when changing from the *anti* to the *syn* isomer.[11c] The difference in chemical shifts between *exo* and *endo* protons at C-24, C-6, and C-21 of diastereomer **1a** (See Scheme 1 for the numbering of atoms), that comprise one half of the *syn–anti* diastereomer **1a**, overlap with the corresponding NMR data from the *syn–syn* diastereomer **1c**, whereas the difference in chemical shifts between *exo* and *endo* protons at C-12, C-18, and C-9, the other half of diastereomer **1a**, exactly matches the corresponding NMR data from diastereomer **1b** (Table 2). Thus, we have completed the assignment of the NMR shifts for diastereomer **1a** vis-à-vis stereochemistry as well. Assignments of individual protons at C-25, C-26, and C-27 were readily made from the COSY spectra showing W-coupling to *endo* protons, such as the coupling between H-25a and H-9 *endo* and between H-25b and H-21 *endo*.

Table 2. Difference in chemical shifts between *exo* and *endo* protons at C-24/12, C-6/18 and C-21/9 for compounds **1a**, **1b**, and **1c**.[a]

Compd	Proton	$\delta_{exo}-\delta_{endo}$ [ppm]	Compd	Proton	$\delta_{exo}-\delta_{endo}$ [ppm]
1a	H-24	0.26	**1c**	H-24/12	0.31
1a	H-6	0.27	**1c**	H-6/18	0.27
1a	H-21	0.52	**1c**	H-21/9	0.61
1a	H-12	0.19	**1b**	H-24/12	0.20
1a	H-18	0.08	**1b**	H-6/18	0.10
1a	H-9	0.39	**1b**	H-21/9	0.34

[a] For the numbering of atoms see Scheme 1.

Isomerization studies of compounds 1a–c: We performed isomerization studies to determine the relative stability of the different diastereomers **1a–c**. Tröger's base is configurationally stable at the stereogenic nitrogen atoms under strongly acidic conditions but not under weakly acidic conditions.[18] Thus, optically pure Tröger's base has been shown to racemize in 0.1 M aqueous HCl within minutes at room temperature.[18a,c] Pardo isomerized the *anti* diastereomer of a nonlinear symmetrically fused bis-Tröger's base analogue

 © 2006 Wiley-VCH Verlag GmbH & Co. KGaA, Weinheim

to a 1:1 mixture of the *anti* and *syn* diastereomers in weak ethanolic HCl at 80 °C after 24 h[11c] but neither the *anti* nor the *syn* diasteromer isomerized in TFA after 48–72 h at room temperature.[12d] Pardo also applied weak ethanolic HCl at 80 °C to the *syn–anti* diastereomer of a nonlinear symmetrically fused tris-Tröger's base 2-methyl-14-nitro-analogue. It isomerized to a 1:2:2:2 mixture of the *anti–anti*, *anti–syn*, *syn–anti*, *syn–syn* diastereomers after 36 h.[12d] Under nonspecified acidic conditions, Král could convert each of all the three possible diastereomers, *syn–anti*, *anti—anti*, and *syn–syn*, of a nonlinear symmetrically fused tris-Trögers base 2,14-dimethoxy-analogue to a mixture containing the starting diastereomer but also the two others.[12b] Finally, we subjected the *syn–anti* and the *anti–anti* diastereomers of a nonlinear symmetrically fused tris-Tröger's base 2,14-dibromo-analogue to TFA at room temperature for several days. In the former case, a 4:1 mixture of *syn–anti* and *anti–anti* resulted and in the latter case no isomerization took place.[12d]

Isomerization studies were conducted using various acidic conditions and temperatures. Each compound **1a–c** was dissolved in concentrated TFA as well as in $CHCl_3$/EtOH (2:1) the latter containing various amounts of 4 M HCl in dioxane, resulting in solutions that were 3, 0.8, and 0.01 M in HCl. The solutions were stirred at 25, 60, and 95 °C. As can be seen from Table 3, the compounds **1a–c** in general are quite surprisingly very stable to isomerization even under forcing reaction conditions. The *syn–anti* isomer does not isomerize at all, not even after 144 h at 95 °C. The *anti–anti* isomer **1b** isomerizes first at 95 °C but to a small extent: 4 and 10 % of the *syn–anti* isomer is formed in 3 and 0.8 M HCl after 144 h, but no isomerization is observed neither in 0.01 M HCl nor in concentrated TFA. In general, the *syn–syn* isomer **1c** isomerizes in the HCl solutions at all investigated temperatures, however only less than 3 % of the *anti–anti* isomer **1b** is obtained after 72 or 144 h. In one case in 3 M HCl at 95 °C, 2 % of the *syn–anti* isomer **1a** was detected in addition to isomer **1b**. In concentrated TFA we detected no isomerization of **1c** at all. Based on this study the *syn–anti* isomer **1a** was slightly more stable than the *anti–anti* **1b** isomer, that was slightly more stable than the *syn–syn* isomer **1c**. However, care must be exercised since the degree of isomerization was very low. More importantly, the observed acidic stability to nitrogen inversion of the fused tris-Tröger′base analogues **1a–c** is unique for Tröger's base analogues to date.

Table 3. Isomerization of **1a–c** under different acidic conditions.[a]

Acid	*T* [°C]	Time [h]	Isomer **1a** product ratio[f] **1a**:**1b**:**1c**	Isomer **1b** product ratio[f] **1a**:**1b**:**1c**	Isomer **1c** product ratio[f] **1a**:**1b**:**1c**
TFA[b]	25	72	100:0:0	0:100:0	0:0:100
3 M HCl[c]	25	72	100:0:0	0:100:0	0:3:97
0.8 M HCl[d]	25	72	100:0:0	0:100:0	0:0:100
0.01 M HCl[e]	25	72	100:0:0	0:100:0	0:2:98
TFA[b]	60	72	100:0:0	0:100:0	0:0:100
3 M HCl[c]	60	72	100:0:0	0:100:0	0:2:98
0.8 M HCl[d]	60	72	100:0:0	0:100:0	0:0:100
0.01 M HCl[e]	60	72	100:0:0	0:100:0	0:2:98
TFA[b]	60	144	100:0:0	0:100:0	0:0:100
3 M HCl[c]	60	144	100:0:0	0:100:0	0:2:98
0.8 M HCl[d]	60	144	100:0:0	0:100:0	0:2:98
0.01 M HCl[e]	60	144	100:0:0	0:100:0	0:2:98
TFA[b]	95	144	100:0:0	0:100:0	0:0:100
3 M HCl[c]	95	144	100:0:0	4:96:0	3:2:95
0.8 M HCl[d]	95	144	100:0:0	10:90:0	0:2:98
0.01 M HCl[e]	95	144	100:0:0	0:100:0	0:0:100

[a] In each experiment, the tris-Tröger's base (5.0 mg, 5.8 μmol) was added to 1.5 mL (in experiment d, 1.87 mL) of the acidic solutions and stirred in sealed tubes. [b] Concentrated TFA. [c] Solution of 4 M HCl in dioxane (7.5 mL, 30 mmol) and $CHCl_3$/EtOH (2:1, 2.5 mL). [d] Solution of 4 M HCl in dioxane (370 μL, 1.48 mmol) and $CHCl_3$/EtOH (2:1, 1.5 mL). [e] Solution of 4 M HCl in dioxane (25 μL, 0.10 mmol) and $CHCl_3$/EtOH (2:1, 9.975 mL). [f] The error of the ratios of products as determined by integrating ^{1}H NMR resonances is estimated to 2 %.

Molecular mechanics calculations show that the *syn–syn* diastereomer **1c** is slightly lower in energy, 2–4 kJ mol^{-1}, than both the *syn–anti* **1a** and the *anti–anti* **1b** isomer. The different diastereomers should, according to their different spatial orientation, be expected to have rather different dipolar moments. It has been noted that for two different nonlinear symmetrically fused bis-Tröger's base analogues, a rather subtle change in the polarity of the substituents in the external ring determines whether the *anti* or *syn* isomer will be the most stable,[11b] supporting the results from the calculations that the difference in energy between the diastereomers in fused Trögers′ base systems is small and might be a result of the different positioning of different functionalized units in **1a–c**. Other important factors that might influence the relative stability of the diastereomers are the choice of solvent (polarity) and the counterion (template effect) of the acid employed.

We believe that the reason why compounds **1a–c** are almost inert to isomerization, compared to the ease with which Tröger's base itself racemizes, is not due to the three-dimensional orientations of isomers **1a–c**, providing locally, sterically hindered environments compared to Tröger's base itself, but due to the presence of substituents in the *ortho*-positions of the aromatic rings fused to the nonaromatic diazocine rings in isomers **1a–c**, that hampers the outside rotation of the intermediate methyl immonium moiety of the diazocine ring, formed after initial protonation of Tröger's base, that is necessary for inverting the absolute configuration of the stereogenic nitrogens in isomers **1a–c**.[18a,27] This conclusion is further supported by the fact that the diastereomers of nonlinear symmetrically fused bis- and tris-Tröger's base analogues, inherently possessing substituents in the *ortho*-positions, are also more stable to isomerization compared to the facile racemization of Tröger's base itself as described above.

Conclusion

For the first time, the *anti–anti* **1a** and the *syn–syn* **1c** diastereomers of a linear symmetrically fused Tröger's base analogue have been isolated, synthesized, and characterized.

 © 2006 Wiley-VCH Verlag GmbH & Co. KGaA, Weinheim

The synthesis methodology developed, based on the use of blocked positions on the aromatic ring and desymmetrization of intermediate C_2-symmetric Tröger's base analogues, will also enable the efficient syntheses of higher generations of linear symmetrically fused Tröger's base analogues. The use of NH_4Cl as an additive in the Tröger's base condensation to diastereomers **1a–c** significantly increased the ratio of the cleft compounds **1a** and **1c** obtained relative to cavity compound **1b**. The clefts of the *syn–anti* **1a** and the *syn–syn* **1c** isomers host solvent molecules in the solid state, as revealed by X-ray diffraction analysis. Uniquely for Tröger's base compounds, the isomers tend not to invert at the stereogenic nitrogens under various acidic conditions and temperatures, most probably due to the presence of the blocking groups on the aromatic rings in the Tröger's base system, hampering the inversion of configuration. Further studies of the compounds **1a–c** will include their host–guest properties, detailed mechanistic explanations of their reluctance to isomerize, the effect of addition of templates in their synthesis, as well as their use in the synthesis of higher generations of linear symmetrically fused Tröger's base analogues.

Experimental Section

General methods: The lithiations were performed in oven-dried glassware under argon by using syringe–septum cap techniques. TLC analyses (Merck 60 F_{254} sheets) were visualized under UV light (254 nm). Column chromatography (CC) was performed on silica gel (Matrex 0.063–0.200 nm), ∅: 3–5 cm, H: 10–20 cm, and fraction size: 20–30 mL. Samples with low solubility in the eluent were dissolved in CH_2Cl_2 or $CHCl_3$, evaporated onto silica, and put on the column as dry powders. Preparative TLC equipment was purchased from Uniplate (silica gel GF, 20×20 cm, 1000 μm). NMR spectra were recorded on a Bruker DRX500 NMR spectrometer at a sample temperature of 300 K, and on Bruker DRX400 or ARX300 NMR spectrometers at a sample temperature of 293 K. Recording of ^{13}C spectra for isomer **1c** was performed at elevated temperature, 310 K, in order to improve line shape for resonances from the inner aromatic ring. Chemical shifts, δ, are reported relative to a shift-scale calibrated with NMR solvent peaks; $CDCl_3$ (7.26 and 77.23 ppm for ^1H and ^{13}C NMR respectively), [D_4]MeOH (3.31 and 49.15 ppm for ^1H and ^{13}C NMR respectively). NMR spectra recording and evaluation of isomers **1a**, **1b**, and **1c** included the use of COSY, HMQC, and HMBC performed with gradient selection, and phase-sensitive NOESY experiments. The HMQC was optimized for $^1J_{C,H}=145$ Hz and the HMBC was optimized for $^nJ_{C,H}=10$ Hz. The NOESY experiment was performed with a mixing-time of 1 s. Scheme 1 shows the numbering of structures and atoms. The ratios between the products yielded in the isomerization studies were determined by integrating the proton resonances in the ^1H NMR spectrum after base-line correction. The error in the integration was estimated at 2%. Melting points were determined in capillary tubes and corrected by using standard substances. Elemental analyses were performed either after CC, preparative TLC, or recrystallization.

Materials: All chemicals were used as received from commercial sources without further purification except for THF that was distilled under argon from sodium benzophenone ketyl and stored over 4 Å molecular sieves. *n*-Butyllithium (*n*BuLi) was titrated prior to use according to the literature.[28] Tosylazide was prepared according a published procedure.[29] 5-Chloro-2-methyl-4-nitroaniline (**2**) was available from Aldrich in technical quality (containing approximately 60% water).

2-Bromo-4-chloro-5-nitrotoluene (3):[20] Aqueous HBr (48% v/v, 7.7 mL) was added to a stirred mixture of 5-chloro-2-methyl-4-nitroaniline (**2**) (5.30 g, technical) and glacial acetic acid (105 mL). $NaNO_2$ (1.96 g, 28.4 mmol) was added in small portions over 1 h. The reaction mixture was heated to 85 °C until no more gas evolved (1.5 h) and was then placed in an ice-bath followed by the addition of H_2O (100 mL) that resulted in the formation of a precipitate. The solid was filtered off and recrystallized from ethanol (99.5%) resulting in a white solid of compound **3** (4.46 g, 17.8 mmol). $R_f=0.26$ (toluene/*n*-heptane (1:4)); m.p. 64–65 °C; ^1H NMR (300 MHz, $CDCl_3$): $\delta=7.80$ (s, 1H), 7.76 (s, 1H), 2.46 ppm (s, 3H); ^{13}C NMR (100 MHz, $CDCl_3$): $\delta=146.5$, 138.7, 135.1, 129.9, 127.1, 125.3, 22.6 ppm; IR (KBr): $\tilde{\nu}=1364$, 1340 cm^{-1} (NO_2); HRMS (EI+): calcd for $C_7H_5NO_2BrCl$: 248.9192; found: 248.9222; elemental analysis calcd (%) for $C_7H_5NO_2BrCl$ (250.5): C 33.57, H 2.01, N 5.59; found: C 33.64, H 1.96, N, 5.65.

4-Bromo-2-chloro-5-methylaniline (4): A suspension of compound **3** (2.93 g, 11.7 mmol), $SnCl_2$ anhydrous (11.0 g, 58.0 mmol), and ethanol (99.5%, 25 mL) was heated at 70 °C under argon. After 1 h, the reaction mixture was allowed to cool to room temperature. The solution was cooled on an ice bath and was then made alkaline (pH 8–10) by the addition of aqueous NaOH (1 M). The resulting slurry was extracted with EtOAc (4×30 mL). The combined organic layers were washed with brine, treated with charcoal, and filtered. The resulting colorless solution was dried over Na_2SO_4, filtered, and evaporated in vacuo, giving a colorless solid of compound **4** in 86% yield (2.32 g, 10.1 mmol). $R_f=0.1$ (EtOAc/*n*-heptane (5:95)); m.p. 77.5–78.3 °C; ^1H NMR (300 MHz, $CDCl_3$): $\delta=7.39$ (s, 1H), 6.65 (s, 1H), 3.98 (s, 2H), 2.28 ppm (s, 3H); ^{13}C NMR (100 MHz, $CDCl_3$): $\delta=142.2$, 137.4, 132.1, 117.6, 117.4, 112.2, 22.6 ppm; IR (KBr): $\tilde{\nu}=3465$, 3377 cm^{-1} (NH_2); HRMS (EI+): calcd for C_7H_7NBrCl: 218.9450; found: 218.9455.

4-Bromo-2-chloro-5-methylaniline·HCl (4·HCl): Aniline **4** (166 mg, 0.663 mmol) was dissolved in chloroform (2 mL) and HCl in dioxane (4 M, 500 μL, 3.00 mmol) was added swiftly resulting in a white precipitate. The mixture was stirred for 20 min and then it was filtered to leave a white solid. The solid was dissolved in dry MeOH (0.5 mL) and precipitated with the addition of Et_2O (7 mL) leaving small, colorless needles of compound **4**·HCl (153 mg, 0.595 mmol). M.p. 77.5–78.3 °C; elemental analysis calcd (%) for $C_7H_8NBrCl_2$ (255.5): C 32.72, H 3.14, N 5.45; found: C 32.72, H 3.08, N 5.40.

2,8-Dibromo-4,10-dichloro-1,7-dimethyl-6*H*,12*H*-5,11-methanodibenzo-[*bf*][1,5]diazocine (5): To a mixture of compound **4** (1.62 g, 7.35 mmol) and paraformaldehyde (451 mg, 15.0 mmol) cooled to −15 °C was added dropwise TFA (15 mL) over 20 min. The reaction mixture was stirred for 26 h in the dark at room temperature. TFA was then removed in vacuo giving a brown oil. The oil was treated first with H_2O (7 mL) giving a pink, gummy solid and then with aqueous NH_3 (28%, 10 mL). The mixture was extracted with CH_2Cl_2 (3×60 mL). The combined organic layers were dried over $MgSO_4$, filtered, and evaporated in vacuo to leave 1.79 g of a pale orange solid. Purification by recrystallization from EtOAc resulted in small, white crystals of compound **5** in 80% yield (1.41 g, 2.96 mmol). $R_f=0.22$ (toluene/CH_2Cl_2 (1:2)); m.p. 261–262 °C; ^1H NMR (400 MHz, $CDCl_3$): $\delta=7.52$ (s, 2H), 4.46 (d, $J=17.8$ Hz, 2H; H-6x and H-12x), 4.27 (d, $J=17.8$ Hz, 2H; H-6n and H-12n), 4.25 (s, 2H), 2.19 ppm (s, 6H); ^{13}C NMR (100 MHz, $CDCl_3$): $\delta=143.0$ (2C), 134.2 (2C), 131.6 (2C), 130.0 (2C), 127.5 (2C), 120.5 (2C), 66.1 (1C), 54.6 (2C), 17.8 ppm (2C); HRMS (EI+): calcd for $C_{17}H_{14}Br_2Cl_2N_2$: 473.8901; found: 473.8901; elemental analysis calcd (%) for $C_{17}H_{14}N_2Br_2Cl_2$ (477.0): C 42.80, H 2.96, N 5.87; found: C 43.13, H 3.00, N 6.23.

2-Azido-8-bromo-4,10-dichloro-1,7-dimethyl-6*H*,12*H*-5,11-methanodibenzo[*bf*][1,5]diazocine (6): To a stirred solution of compound **5** (416 mg, 0.872 mmol) in anhydrous THF (30 mL) at −78 °C was added dropwise 2.28 M *n*BuLi in hexane (415 μL, 0.946 mmol) over 3 min giving a dark red solution. After 5 min, tosylazide (200 μL, 1.30 mmol) was added dropwise over 30 s and then the reaction mixture was allowed to reach room temperature. After 18 h the reaction was quenched by the addition of water (10 mL). The layers were separated and the aqueous phase was further extracted with CH_2Cl_2 (3×20 mL). The combined organic layers were dried over $MgSO_4$, filtered, and evaporated in vacuo

 © 2006 Wiley-VCH Verlag GmbH & Co. KGaA, Weinheim

leaving a thick, brown oil. CC on the crude product (*n*-heptane/CH_2Cl_2-(5:95)) gave 81% yield of compound **6** (224 mg, 0.510 mmol) as a pale-yellow solid. R_f=0.23 (*n*-heptane/CH_2Cl_2(5:95)); ^{1}H NMR (400 MHz, $CDCl_3$): δ=7.52 (s, 1H), 7.09 (s, 1H), 4.46 (d, J=17.6 Hz, 1H; H-6x), 4.41 (d, J=17.6 Hz, 1H; H-12x), 4.26 (d, J=17.2 Hz, 1H; H-6n), 4.25 (s, 2H; H-13), 4.23 (d, J=18.4 Hz, 1H; H-12n), 2.19 (s, 3H), 1.97 ppm (s, 3H); ^{13}C NMR (100 MHz, $CDCl_3$): δ=143.11, 140.47, 135.10, 134.26, 131.61, 130.18, 130.13, 127.66, 127.57, 126.12, 120.49, 117.99, 66.32, 54.86, 54.11, 17.78, 11.95 ppm; HRMS (FAB+): calcd for $C_{17}H_{14}BrCl_2N_5$: 436.9810; found: 436.9811.

2-Amino-8-bromo-4,10-dichloro-1,7-dimethyl-6*H*,12*H*-5,11-methanodibenzo[*b*,*f*][1,5]diazocine (7): To a solution of compound **7** (487 mg, 1.11 mmol) in anhydrous THF (40 mL) was added $NaBH_4$ (210 mg, 6.99 mmol) in small portions at room temperature. The mixture was heated to reflux and MeOH (1.1 mL) was added dropwise over 50 min. After refluxing for 4 h, the reaction mixture was allowed to come to room temperature. Concentrated HCl (37%, 2 mL) was added giving a white precipitate. The reaction mixture was made alkaline (pH 10) by using aqueous NaOH (10 M) at 0°C. H_2O (10 mL) was added. The layers were separated and the aqueous layer was extracted with EtOAc. The combined organic layers were dried over $MgSO_4$, filtered, and evaporated in vacuo to give 510 mg of a yellow solid. CC (EtOAc/*n*-heptane (15:85) gave a white solid of compound **7** in 93% yield (430 mg, 1.04 mmol). R_f=0.21 (EtOAc/*n*-heptane (15:85)); m.p. 190–192°C; ^{1}H NMR (400 MHz, $CDCl_3$): δ=7.51 (s, 1H), 6.70 (s, 1H), 4.17–4.50 (m, 6H), 3.50 (s, 2H), 2.18 (s, 3H), 1.90 ppm (s, 3H); ^{13}C NMR (100 MHz, $CDCl_3$): δ=143.4. 141.9, 134.9, 134.2, 131.3, 130.6, 128.7, 127.4, 127.1, 120.2, 118.1, 115.4, 66.4, 55.0, 54.3, 17.8, 11.5 ppm; IR (KBr): $\tilde{\nu}$=3456, 3352 cm^{-1} (NH_2); HRMS (FAB+): calcd for $C_{17}H_{16}BrCl_2N_3$: 410.9905; found: 410.9907.

2-Amino-8-bromo-4,10-dichloro-1,7-dimethyl-6*H*,12*H*-5,11-methanodibenzo[*b*,*f*][1,5]diazocine·HCl (7·HCl): Compound **7** (50 mg, 0.12 mmol) was dissolved in the smallest amount possible of CH_2Cl_2 (4 mL) and HCl in dioxane (4 M, 500 μL, 2 mmol) was added swiftly resulting in a white precipitate. The solid was filtered and dissolved in the smallest amount possible of MeOH (1 mL) and then Et_2O (8 mL) was added resulting in a precipitate. The mixture was filtered, washed with cold Et_2O, and dried to give a white solid of **7**·HCl (43 mg, 0.096 mmol). Elemental analysis calcd (%) for $C_{17}H_{17}BrCl_3N_3$ (449.6): C 45.41, H 3.81, N 9.35; found: C 45.36, H 3.74, N 9.27.

2,14-Dibromo-4,10,16,22-tetrachloro-1,7,13,19-tetramethyl-9*H*,21*H*-8,20-methanobis(6*H*,12*H*-5,11-methanodibenzo[*b*,*f*][1,5]diazocine)[*b*-2,3;*f*-8′,9′][1,5]diazocine (1): To a mixture of compound **7** (430 mg, 1.04 mmol) and paraformaldehyde (80 mg, 2.7 mmol) at −10°C, TFA (3 mL) was added dropwise over 20 min. After the addition of TFA, the reaction mixture was allowed to come to room temperature and the resulting solution was stirred in the dark for 72 h. TFA was removed in vacuo, resulting in a brown oil. H_2O (5 mL) was added to this oil followed by saturated aqueous NH_3 (28%, 4 mL), resulting in a pink gummy solid. The reaction mixture was first extracted with CH_2Cl_2 (2×10 mL), and then with $CHCl_3$ (3×5 mL). The combined $CHCl_3$ layers were dried over $MgSO_4$, filtered, and evaporated under reduced-pressure to give compound **1b** as a white solid in 13% yield (64 mg, 0.074 mmol). The same procedure was followed with the combined CH_2Cl_2 layers, giving a pale yellow solid. CC (EtOAc/CH_2Cl_2 (5:95)) gave compounds **1a** and **1c** as separate fractions, and a mixed fraction of compounds **1a**, **1b**, and **1c** (66 mg, 0.076 mmol). The combined fractions containing each of compounds **1a** and **1c**, respectively, were evaporated to dryness in vacuo. The mixed fraction was not further purified due to its low solubility in the eluent. Compound **1a** was reprecipitated by dissolving it in the smallest amount possible of $CHCl_3$ followed by addition of Et_2O giving pure compound **1a** as a white solid in 32% yield (157 mg, 0.182 mmol). Compound **1c** was further purified twice by preparative TLC (EtOAc/$CHCl_3$ (15:85)) giving pure compound **1c** as a white solid in 8% yield (28 mg, 0.032 mmol).

Compound 1a: R_f=0.33 (EtOAc/CH_2Cl_2 (5:95)); m.p.>400°C (darkened at about 250°C); ^{1}H NMR (500 MHz, $CDCl_3$): δ=7.51 (s, 1H; H-15), 7.49 (s, 1H; H-3), 4.46 (d, J=17 Hz, 1H; H-6x), 4.44 (d, J=17 Hz, 1H; H-21x), 4.40 (d, J=17 Hz, 2H; H-12x/H-24x), 4.36 (d, J=17 Hz, 1H; H-18x), 4.32 (d, J=18 Hz, 1H; H-9x), 4.29 (d, J=13 Hz, 1H; H-25b), 4.28 (d, J=18 Hz, 1H; H-18n), 4.24 (d, J=13 Hz, 1H; H-25a), 4.21 (d, J=17 Hz, 1H; H-12n), 4.20 (d, J=17 Hz, 1H; H-6n), 4.19 (d, J=13 Hz, 1H; H-26a), 4.17 (d, J=14 Hz, 1H; H-27a), 4.14 (d, J=17 Hz, 1H; H-24n), 4.12 (d, J=14 Hz, 1H; H-27b), 4.10 (d, J=13 Hz, 1H; H-26b), 3.93 (d, J=17 Hz, 1H; H-9n), 3.92 (d, J=18 Hz, 1H; H-21n), 2.21 (s, 3H; Me-7), 2.20 (s, 3H; Me-19), 2.17 (s, 3H; Me-13), 2.14 ppm (s, 3H; Me-1); ^{13}C NMR (125 MHz, $CDCl_3$): δ=143.75 (C-19a), 143.66 (C-7a), 143.38 (C-16a), 143.24 (C-4a), 139.79 (C-22a), 139.59 (C-10a), 134.17 (C-13), 134.04 (C-1), 131.53 (C-3), 131.51 (C-15), 130.38 (C-12a), 130.35 (C-24a), 129.36 (C-19), 129.31 (C-7), 127.57 (C-16), 127.50 (C-4), 127.50 (C-6a), 127.41 (C-18a), 125.72 (C-10), 125.35 (C-22), 125.22 (C-21a), 124.88 (C-9a), 120.43 (C-2), 120.37 (C-14), 66.61 (C-26), 66.56 (C-25), 66.30 (C-27), 55.03 (C-21), 54.78 (C-9), 54.74 (C-24), 54.74 (C-12), 54.19 (C-6), 54.02 (C-18), 17.73 (Me-13), 17.71 (Me-1), 11.98 (Me-7), 11.81 ppm (Me-19); HRMS (FAB+): calcd for $C_{37}H_{32}Br_2C_{l4}N_6$: 857.9809; found: 857.9790; elemental analysis calcd (%) for $C_{37}H_{32}Br_2Cl_4N_6$ (862.3): C 51.54, H 3.74, N 9.75; found: C 51.62, H 3.67, N 9.66.

Compound 1b: R_f=0.23 (EtOAc/CH_2Cl_2 (5:95)); m.p.>400°C (darkened at about 250°C); ^{1}H NMR (500 MHz, $CDCl_3$): δ=7.52 (s, 2H; H-3/15), 4.43 (d, J=17 Hz, 2H; H-12x/24x), 4.40 (d, J=17 Hz, 2H; H-6x/18x), 4.37 (d, J=18 Hz, 2H; H-9x/21x), 4.30 (d, J=17 Hz, 2H; H-6n/18n), 4.24 (d, J=17 Hz, 2H; H-12n/24n), 4.22 (d, J=13 Hz, 2H; H-25a/27a), 4.19 (d, J=13 Hz, 2H; H-25b/27b), 4.09 (s, 2H; H-26), 4.03 (d, J=18 Hz, 2H; H-9n/21n), 2.22 (s, 6H; Me-7/Me-19), 2.18 ppm (s, 6H; Me-1/Me-13); ^{13}C NMR (125 MHz, $CDCl_3$): δ=143.74 (C-7a/19a), 143.46 (C-4a/16a), 139.76 (C-10a/22a), 134.18 (C-1/13), 131.51 (C-3/15), 130.38 (C-12a/24a), 129.24 (C-7/19), 127.59 (C-4/16), 127.46 (C-6a/18a), 125.43 (C-10/22), 125.08 (C-9a/21a), 120.36 (C-2/14), 66.37 (C-26), 66.31 (C-25/27), 54.97 (C-9/21), 54.77 (C-12/24), 54.08 (C-6/18), 17.75 (Me-1/Me-13), 11.84 ppm (Me-7/Me-19); HRMS (FAB+): calcd for $C_{37}H_{32}Br_2C_{l4}N_6$: 857.9809; found: 857.9809.

Compound 1c: R_f=0.20 (EtOAc/CH_2Cl_2 (5:95)); m.p.>400°C (darkened at about 250°C); ^{1}H NMR (500 MHz, $CDCl_3$): δ=7.50 (s, 2H; H-3/15), 4.47 (d, J=17 Hz, 2H; H-6x/18x), 4.45 (d, J=17 Hz, 2H; H-9x/21x), 4.39 (d, J=17 Hz, 2H; H-12x/24x), 4.25 (d, J=12 Hz, 2H; H-25b/27b), 4.20 (d, J=12 Hz, 2H; H-25a/27a), 4.19 (d, J=17 Hz, 2H; H-6n/18n), 4.18 (s, 2H; H-26), 4.08 (d, J=17 Hz, 2H; H-12n/24n), 3.84 (d, J=17 Hz, 2H; H-9n/21n), 2.21 (s, 2H; Me-7/Me-19), 2.08 ppm (s, 2H, Me-1/Me-13); ^{13}C NMR (125 MHz, $CDCl_3$, 310 K): δ=143.59 (C-7a/19a), 143.39 (C-4a/16a), 139.92 (C-10a/22a), 134.22 (C-1/13), 131.57 (C-3/15), 130.21 (C-12a/24a), 129.69 (C-7/19), 127.76 (C-4/16), 127.32 (C-6a/18a), 125.42 (C-10/22), 125.39 (C-9a/21a), 120.51 (C-2/14), 66.78 (C-26), 66.55 (C-25/27), 54.74(C-9/21), 54.68 (C-12/24), 54.18 (C-6/18), 17.74 (Me-1/Me-13), 11.93 ppm (Me-7/Me-19); HRMS (FAB+): calcd for $C_{37}H_{32}Br_2C_{l4}N_6$: 857.9809; found: 857.9812.

Isomerizations

General Procedure 1: The isomers, *syn–anti* **1a**, *anti–anti* **1b**, and *syn–syn* **1c** (5 mg, 5.8 μmol) were dissolved in TFA (1 mL) in three separate flasks and the flasks were sealed. The resulting solutions were stirred for 72 or 144 h. To each reaction mixture was added water (2 mL) and the resulting mixture was then made alkaline by the addition of saturated aqueous NH_3 (28%). The mixture was extracted with $CHCl_3$ (3×5 mL) and the combined organic layers were washed with water, dried over $MgSO_4$, filtered, and evaporated.

Condition 1A: 72 h at RT. No isomerization occurred for any of the three isomers.

Condition 1B: 72 h at 60°C. No isomerization occurred for any of the three isomers.

Condition 1C: 144 h at 60°C. No isomerization occurred in any of the three isomers.

Condition 1D: 144 h at 95°C. No isomerization occurred in any of the three isomers.

General Procedure 2: The isomers, *syn–anti* **1a**, *anti–anti* **1b**, and *syn–syn* **1c** (5 mg, 5.8 μmol) were dissolved in TFA (1 mL) in three separate flasks and the flasks were sealed. The solutions were stirred for 72 or 144 h. To each reaction mixture was added water (2 mL) and the result-

 © 2006 Wiley-VCH Verlag GmbH & Co. KGaA, Weinheim

ing mixture was then made alkaline by saturated aqueous NH_3 (28%). The mixture was extracted with $CHCl_3$ and the combined organic layers were washed with water, dried over $MgSO_4$, filtered, and evaporated.

Condition 2A: 3 M HCl, 72 h at room temperature. Isomers **1a** and **1b** did not isomerize. Isomer **1c** gave a mixture of **1c** and **1b** in a 97:3 ratio.

Condition 2B: 0.8 M HCl, 72 h at RT. No isomerization occurred for any of the three isomers.

Condition 2C: 0.01 M HCl, 72 h at room temperature. Isomers **1a** and **1b** did not isomerize. Isomer **1c** gave a mixture of **1c** and **1b** in a 98:2 ratio.

Condition 2D: 3 M HCl, 72 h at 60 °C. Isomers **1a** and **1b** did not isomerize. Isomer **1c** gave a mixture of **1c** and **1b** in a 98:2 ratio.

Condition 2E: 0.8 M HCl, 72 h at 60 °C. No isomerization occurred for any of the three isomers.

Condition 2F: 0.01 M HCl, 72 h at 60 °C. Isomers **1a** and **1b** did not isomerize. Isomer **1c** gave a mixture of **1c** and **1b** in a 98:2 ratio.

Condition 2G: 3 M HCl, 144 h at 60 °C. Isomers **1a** and **1b** did not isomerize. Isomer **1c** gave a mixture of **1c** and **1b** in a 98:2 ratio.

Condition 2H: 0.8 M HCl, 144 h at 60 °C. Isomers **1a** and **1b** did not isomerize. Isomer **1c** gave a mixture of **1c** and **1b** in a 98:2 ratio.

Condition 2I: 0.01 M HCl, 144 h at 60 °C. Isomers **1a** and **1b** did not isomerize. Isomer **1c** gave a mixture of **1c** and **1b** in a 98:2 ratio.

Condition 2J: 3 M HCl, 144 h at 95 °C. Isomer **1a** did not isomerize. Isomer **1b** gave a mixture of **1b** and **1a** in a 96:4 ratio. Isomer **1c** gave a mixture of **1c**, **1a**, and **1b** in a 95:3:2 ratio.

Condition 2K: 0.8 M HCl, 144 h at 95 °C. Isomer **1a** did not isomerize. Isomer **1b** gave a mixture of **1b** and **1a** in a 90:10 ratio. Isomer **1c** gave a mixture of **1c** and **1b** in a 98:2 ratio.

Condition 2L: 0.01 M HCl, 144 h at 95 °C. No isomerization occurred for any of the three isomers.

Preparation of the HCl solutions: The 3 M HCl solution was prepared from 4 M HCl in dioxane (7.5 mL, 30 mmol) and $CHCl_3$/EtOH (2:1, 2.5 mL). The 0.8 M HCl solution was prepared from 4 M HCl in dioxane (370 μL, 1.48 mmol) and $CHCl_3$/EtOH (2:1, 1.5 mL). The 0.01 M HCl solution was prepared from 4 M HCl in dioxane (25 μL, 0.10 mmol) and $CHCl_3$/EtOH (2:1, 9.975 mL).

Molecular modeling: The molecular modeling of the fused hepta-Tröger's base analogues was performed by using the program MacroModel Version 8.5[30] and the energy was minimized by using the MM3* force-field.[30,31] The calculations of the relative energies of isomers **1a**:**1b**:**1c** were carried out by using both MM3* and MMFFs[32] force-fields in vacuo and with the built-in solvation model for water.

X-ray diffraction analysis: Crystal data and details about data collection are given in Table 4. The intensity data sets for compounds **1a**·2 CH_2Cl_2 and **1c**·C_3 (the disordered solvent molecules are tentatively labeled C_3) were collected at 293 K with a Bruker SMART 1000 CCD system[33] by using ω-scans and synchrotron radiation at MAXLAB II, Lund, Sweden ($\lambda = 0.89742$ Å for **1a**·2 CH_2Cl_2 and 0.910 Å for **1c**·C_3).[34] CCD data were extracted and integrated by using Twinsolve.[35] Both structures were solved by direct methods and refined by full-matrix least-squares calculations on F^2 by using SHELXTL Version 5.1.[36] For **1a**·2 CH_2Cl_2, non-hydrogen atoms were refined with anisotropic displacement parameters. Hydrogen atoms were constrained to parent sites, by using a riding model. The highest residual electron density is situated close to CL7 in the dichloromethane molecule (omitted in Figure 4). The crystals of **1c**·C_3 were weak scatterers also by using synchrotron irradiation giving rise to poor data and a high value of R_{int}.[37] Thus, only the halogen atoms were refined anisotropically. In the cavity formed by the molecules there was residual electron density probably due to the presence of disordered solvent molecules. No chemically sensible structure of this molecule could be obtained and it was modeled by using three isotropic carbon atoms (C101–103, also labeled C_3). The highest residual electron density is close to atom C1B. The poor quality of the **1c**·C_3 structure precludes any detailed conclusions on the quantitative aspects of the structure, but the data unambiguously proves the molecular structure of isomer **1c** to be the *syn–syn* diastereomer, as well as the qualitative aspects about its aggregation and inclusion properties in the solid state as outlined above.

Table 4. Crystal data for compounds **1a**·2 CH_2Cl_2 and **1c**·C_3.

	1a·2 CH_2Cl_2	**1c**·C_3
chemical formula	$C_{37}H_{32}Br_2Cl_4N_6$·CH_2Cl_2	$C_{37}H_{32}Br_2Cl_4N_6$·C_3
M_w [g mol^{-1}]	1032.16	898.34
crystal system	triclinic	monoclinic
space group	$P\bar{1}$	$P2/n$
a [Å]	9.2983(19)	21.022(4)
b [Å]	12.921(3)	9.0223(18)
c [Å]	17.529(4)	25.161(5)
α [°]	99.07(3)	90
β [°]	92.64(3)	113.08(3)
γ [°]	90.23(3)	90
V [Å^3]	2077.3(7)	4390.2(15)
Z	2	4
ρ_{calcd} [g cm^{-3}]	1.650	1.359
μ [mm^{-1}]	2.504	2.124
θ range	1.49–31.98	2.25–32.63
collected reflections	8579	13413
unique reflections	6409 ($R_{int} = 0.2517$)	7082 ($R_{int} = 0.3187$)
no of parameters	497	237
$R(F)$[a], $wR(F^2)$[b] ($I > 2\sigma(I)$)	0.1173, 0.3694	0.2924, 0.5024
$wR(F^2)$ (all data)	0.3849	0.5405
S[c]	1.798	1.676
residual e-density [e Å^{-3}]	2.038	1.609

[a] $R = \Sigma(|F_o|-|F_c|)/\Sigma|F_o|$. [b] $wR = [\Sigma w(|F_o|-|F_c|)^2/\Sigma|F_o|^2]^{1/2}$. [c] $S = [\Sigma w(|F_o|-|F_c|)^2/(m-n)]^{1/2}$.

CCDC 284529 (**1a**) and 284530 (**1c**) contain the supplementary crystallographic data for this paper. These data can be obtained free of charge from the Cambridge Crystallographic Data Centre via www.ccdc.cam.ac.uk/data_request/cif.

Acknowledgements

We thank Peter Fristrup from the Technical University of Denmark for help with molecular modeling. The Crafoord Foundation, the Swedish Research Council (O.F.W.) and the Swedish Foundation for Strategic Research are acknowledged for financial support. MAXLAB in Lund is acknowledged for beam time.

[1] A. J. Marmur, *J. Am. Chem. Soc.* **2000**, *122*, 2120–2121.
[2] J. W. Steed, J. L. Atwood, *Supramolecular Chemistry*, Wiley, Chichester, England, **2000**, p. 28.
[3] a) C. A. Hunter, J. K. M. Sanders, *J. Am. Chem. Soc.* **1990**, *112*, 5525–5534; b) S. Paliwal, C. S. Wilcox, *J. Am. Chem. Soc.* **1994**, *116*, 4497–4498; c) E. Kim, S. Paliwal, C. S. Wilcox, *J. Am. Chem. Soc.* **1998**, *120*, 11192–11193; d) C. A. Hunter, P. S. Jones, P. Tiger, S. Tomas, *Chem. Eur. J.* **2002**, *8*, 5435–5446.
[4] J. C. Ma, D. Dougherty, *Chem. Rev.* **1997**, *97*, 1303–1324.
[5] F.-G. Klärner, J. Panitzsky, D. Bläser, R. Boese, *Tetrahedron* **2001**, *57*, 3673–3687.
[6] a) C.-W. Chen, H. W. Whitlock, *J. Am. Chem. Soc.* **1978**, *100*, 4921–4922; b) S. C. Zimmerman, C. M. vanZyl, *J. Am. Chem. Soc.* **1987**, *109*, 7894–7896; c) R. P. Sijbesma, A. P. M. Kentgens, R. J. M. Nolte, *J. Org. Chem.* **1991**, *56*, 3199–3201; d) A. Rowan, J. A. A. W. Elemans, R. J. M. Nolte, *Acc. Chem. Res.* **1999**, *32*, 995–1000; e) F.-G. Klärner, J. Benkhoff, J. Boese, U. Burkert, M. Kamieth, *Angew. Chem.* **1996**, *108*, 1195–1198; *Angew. Chem. Int. Ed. Engl.* **1996**, *35*, 1130–1133; f) F.-G. Klärner, B. Kahlert, *Acc. Chem. Res.* **2003**, *36*, 919–932; g) H. Kurebayashi, T. Haino, S. Usui, Y. Fukazawa, *Tetrahedron* **2001**, *57*, 8667–8674.

 © 2006 Wiley-VCH Verlag GmbH & Co. KGaA, Weinheim

[7] a) M. Harmata, C. L. Barnes, *Tetrahedron Lett.* **1990**, *31*, 1825–1828; b) M. Harmata, *Acc. Chem. Res.* **2004**, *37*, 862–873.
[8] J. Tröger, *J. Prakt. Chem.* **1887**, *36*, 225–245.
[9] For recent reviews see: a) M. Vali′k, R. M. Strongin, V. Král, *Supramol. Chem.* **2005**, *17*, 347–367; b) M. Demeunynck, A. Tatibouët, *Progress in Heterocyclic Chemistry, Vol. 11*, (Eds.: G. W. Gribble, T. L. Gilchrist), Pergamon, Oxford, England, **1999**, pp. 1–20.
[10] C. S. Wilcox, L. M. Greer, V. Lynch, *J. Am. Chem. Soc.* **1987**, *109*, 1865–1867.
[11] a) C. Pardo, E. Sesmilo, E. Gutiérrez-Puebla, A. Monge, J. Elguero, A. Fruchier, *J. Org. Chem.* **2001**, *66*, 1607–1611; b) M. Valík, B. Dolensky′, H. Petricková, V. Král, *Collect. Czech. Chem. Commun.* **2002**, *67*, 609–621; c) T. Mas, C. Pardo, F. Salort, J. Elguero, M. R. Torres, *Eur. J. Org. Chem.* **2004**, 1097–1104.
[12] a) T. Mas, C. Pardo, J. Elguero, *Mendeleev Commun.* **2004**, 235–237; b) B. Dolensky′, M. Valík, D. Sy′kora, V. Král, *Org. Lett.* **2005**, *7*, 67–70; c) A. Hansson, T. Wixe, K.-E. Bergquist, K. Wärnmark, *Org. Lett.* **2005**, *7*, 2019–2022; d) T. Mas, C. Pardo, J. Elguero, *Helv. Chim. Acta* **2005**, *88*, 1199–1207.
[13] The names of the regioisomers refer to the symmetry of the carbon skeleton without substituents as defined in reference [12c].
[14] a) The names of the diastereomers refer to the relative position of the NCH_2N moieties in each diastereomer as defined in references [11a, 12a]; b) For the nonsymmetric regioisomer there is a possibility of an *anti–syn* diastereomer as well. See references [12a, 12d].
[15] Making extended fused Tröger's base analogues of tubular-shape by fusing two nonlinear symmetrically fused tris-Tröger's base analogues is impossible as revealed by molecular modelling (see Experimental Section for technical details).
[16] For an up-to-date review on organic nanotubes see: M. A. B. Block, C. Kaiser, A. Khan, S. Hecht, *Top. Curr. Chem.* **2005**, *245*, 89–150.
[17] Král isolated the *syn–anti* diastereomer of a linear symmetrically fused tris-Tröger's base analogue from a complex mixture of poly-Tröger's base analogues by blocking one of the *ortho*-positions of the aniline monomer. See reference [12b].
[18] a) V. Prelog, P. Wieland, *Helv. Chim. Acta* **1944**, *27*, 1127–1134; b) A. Greenberg, N. Molinaro, M. Lang, *J. Org. Chem.* **1984**, *49*, 1127–1130; c) one exception is an acridine analogue which, due to the preferable protonation of the acridine moiety, leaves the Tröger's base nitrogen atoms unprotonated: A. Tatibouët, M. Demeunynck, C. Andraud, A. Collet, J. Lhomme, *Chem. Commun.* **1999**, 161–162.
[19] Independently, by using a different approach, Pardo also synthesized an *anti–anti* diastereomer of a fused tris-Tröger's base analogue, see reference [12d].
[20] Compound **3** has previously been synthesized from *p*-nitrotoluene in six steps: J. P. Lambooy, *Proc. Soc. Exp. Biol. Med.* **1972**, *141*, 948–952.
[21] a) J. Jensen, K. Wärnmark, *Synthesis* **2001**, 1873–1877; b) J. Jensen, M. Strozyk, K. Wärnmark, *J. Heterocycl. Chem.* **2003**, *40*, 273–375.
[22] a) We have previously shown that the temperature of the reaction mixture when TFA is added influences the yield in the Tröger's base condensation of halogen-substituted anilines: reference [21b]; b) this protocol has been improved during the present work by Diederich and co-workers: S. Sergeyev, M. Schär, P. Seiler, O. Lukoyanova, L. Echegoyen, F. Diederich, *Chem. Eur. J.* **2005**, *11*, 2284–2294.
[23] S. B. Larson, C. S. Wilcox, *Acta Crystallogr. Sect. C* **1986**, *42*, 224–227.
[24] K. Brandenburg, DIAMOND, Program for Molecular Graphics: Crystal Impact, Bonn, Germany, **2000**.
[25] G. R. Desiraju, T. Steiner, *The Weak Hydrogen Bond*, IUCr Monographs on Crystallography 9, Oxford University Press, England, **1999**.
[26] J. Elguero, A. Fruchier, T. Mas, and C. Pardo, *Magn. Reson. Chem.* **2005**, *43*, 665–669.
[27] Inspection of molecular models shows that the space inside the diazocine ring methyl immonium intermediate, the key intermediate in the acidic racemization of Tröger's base (see ref. [18b]), is too small to allow the rotation of the methyl immonium part inside the eight-membered ring.
[28] E. Juaristi, A. Martinez-Richa, A. Garcia-Rivera, J. S. Cruz-Sanchez, *J. Org. Chem.* **1983**, *48*, 2603–2606.
[29] A. K. Ghosh, A. Bischoff, J. Cappiello, *Eur. J. Org. Chem.* **2003**, 821–832.
[30] MacroModel Version 8.5 from Schrödinger Inc. , F. Mohamadi, N. G. J. Richards, W. C. Guida, R. Liskamp, M. Lipton, C. Caulfield, G. Chang, T. Hendrickson, W. C. Still, *J. Comput. Chem.* **1990**, *11*, 440–467.
[31] N. L. Allinger, Y. H. Yuh, J.-H. Lii, *J. Am. Chem. Soc.* **1989**, *111*, 8551–8566.
[32] T. A. Halgren, *J. Comput. Chem.* **1996**, *17*, 490–519.
[33] Bruker AXS, SMART, Area Detector Control Software, Bruker Analytical X-ray System, Madison WI, USA, **1995**.
[34] Y. S. Cerenius, K. Ståhl, L. A. Svensson, T. Ursby, Å. Oskarsson, J. Albertsson, A. J. Liljas, *J. Synchrotron Radiat.* **2000**, *7*, 203–208.
[35] TwinSolve (2004), A Program for the Deconvolution and Processing of Rotation Twins′, RigakuMSC Inc. and Prekat AB (c), **1998–2004**.
[36] G. M. Sheldrick, SHELXTL, Version 5.1, Program for Structure Solution and Least-Squares Refinement, University of Göttingen, Göttingen, Germany, **1998**.
[37] M. S. Weiss, R. Hilgenfeld, *J. Appl. Crystallogr.* **1997**, *30*, 203–205.

Received: September 23, 2005
Published online: January 23, 2006

 © 2006 Wiley-VCH Verlag GmbH & Co. KGaA, Weinheim